Double Inverted Pendulum Dynamics

by Devin Johnson, Zach Kirch

Mentor: Kevin Luna

Introduction:

For this project, our goal centered around understanding the dynamics and general motion of a Double Inverted Pendulum (DIP) system. We wanted to construct the general equations of motion of the DIP system, producing the Lagragian of the system and equations that determined the general stability of the system. This system, however, is a chaotic system that does not have an analyzable Effective Potential associated with it, hindering our ability to quantify exact stable points of the system. Additionally, points that are just slightly translated from a stable position can cause vastly different motions of the two arms. These factors made it extremely hard to produce known stable points of the DIP system, so we attempted to analyze the problem with a more generalized, surface level approach. We studied the different motions in the system with varying lengths of the two arms, varying masses at the two ends, and varying amplitudes and frequencies of the oscillation at the base. From these results, we obtained data that allowed us to postulate the general dynamics of the system, and what range of initial configurations the stable points may be located within.
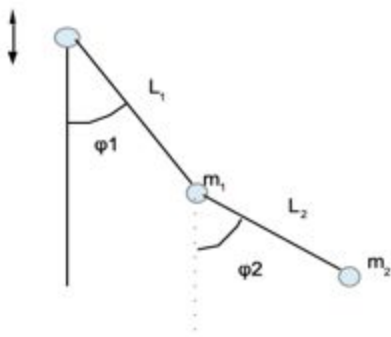
These results could help in the future production of a process to analyze the stable points of the DIP system. With this type of procedure in place, the estimation and control algorithms could be improved upon even further, and these same algorithms could then be applied to much more advanced mechatronic systems.

Figure 1. Diagram of DIP

Applications:

The DIP system is indeed a crucial system in the field of control research, as it is a generally simple system to build and test. This means that certain estimation models that are applied to the system can be verified on a physical system, and these same estimation models can be applied to various other, more complex mechanical systems.

As mentioned before, this is a chaotic motion system, meaning that if the two arms are not placed at the exact locations of stability within the system, it can exhibit a wildly different path of motion. In this way, this system is incredibly hard to analyze for points of stability. Therefore, many estimates and assumptions have to be made to produce equations of motion that can be decomposed and produce concrete stability points.

One important field of study is applying different self-correcting algorithms within controllers that can keep the DIP system in a state of constant stability. There have been countless number of research projects that implement controllers that allow the system to stay within a state of equilibrium. But many of them analyze systems that have key differences to the one we chose, including different base systems or different motions of the base. However, these papers gave us a better understanding of how our findings could be applied to similar research projects.
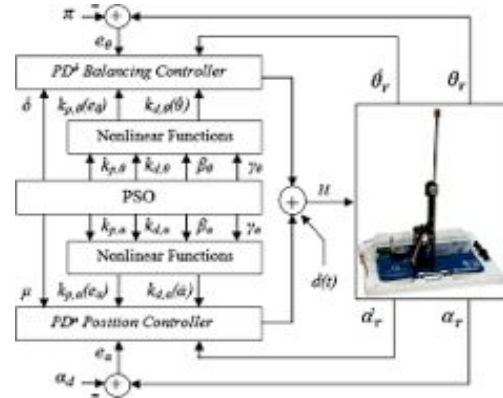
Figure 2. Complex Mechatronic system using Estimation of DIP

Producing the various plots and finding ranges where potential stable points would occur also would be beneficial to the various controllers produced for the purpose of studying the physical DIP system. With the added information we obtained by testing various lengths and masses of the DIP, and various base oscillation parameters, we gained a better understanding of which types of systems had stable points that were easier to identify, or which systems were so chaotic that a stable point could not be found. These findings could be applied to future research papers to tailor the system design for these different goals, of potentially building a highly chaotic system to try to find estimation strategies that adequately produced stable nodes, or of producing systems with easier to analyze stability points to model mechanical systems that more so reflect this design.

Theory:

Similar to the Midterm, the primary initial goal was in understanding the system such that the equations for the x and y coordinates could be expressed in terms of a Polar coordinate system, and then using these in the Kinetic and Potential Energy equations to eventually obtain Lagrangian Equations of Motion.

As in the Midterm, an Origin point O was selected at the initial base location of the system. From there, a rod of length l_1 with a ball attached at the end of it, carrying a weight of m_1 was attached to this base. Additionally, a second rod of length l_2 with a ball attached at the end of it, carrying a weight of m_2 was attached to the end of the first Pendulum arm. The rods were assumed to have a negligible mass, and were not factored into the equations of motion.

Based on this setup, we were able to easily translate the (x, y) Cartesian coordinate of the ends of both rods into their respective Polar coordinates. This was done because it reduced the total number of equations by a factor of two, as there were only the corresponding values of ϕ_1 and ϕ_2 to solve for, instead of generating equations for all of x_1, y_1, x_2 and y_2.

Another important note to point out is how we chose to define the two angles ϕ_1 and ϕ_2, as there were two major ways in which we could define them. The first we analyzed was defining ϕ_1 with respect to the vertical line extended from the base, and defining ϕ_2 with respect to the line extended from the first rod. These equations resulted in very tedious and long equations of motion. The other definition of these angles, however, resulted in more manageable equations to solve for. This was when ϕ_1 was defined in the same manner, but ϕ_2 was defined by the angle made with an imaginary line that ran from the first mass parallel to the initial base rod. This was the manner in which we chose to define our two angles ϕ_1 and ϕ_2, as both ways allowed us to understand the movements of both arms of the system.

In the section below, the Lagrangian Equation and the resulting Equations of Motion were derived based on our definition of the system as laid out in this Theory section.

Lagrangian and Equations of Motion:

As in the Midterm paper, we derived the Equations of motion based on the initial equations obtained for x and y:

$$x_1 = l_1 sin(\phi_1)$$
$$y_1 = l_1 cos(\phi_1) + a\, cos(\Omega t)$$
$$x_2 = l_1 sin(\phi_1) + l_2 sin(\phi_2)$$
$$y_2 = l_1 cos(\phi_1) + l_2 cos(\phi_2) + a\, cos(\Omega t)$$

X/Y Equations Set

It then follows that the equations for the Kinetic Energy and Potential Energy are:

$$T = \frac{m_1[(x_1')^2 + (y_1')^2]}{2} + \frac{m_2[(x_2')^2 + (y_2')^2]}{2}$$

$$U = -m_1 g y_1 - m_2 g y_2$$
$$L = T - U$$

Substituting the expressions in the *X/Y Equations Set* into the terms found in the *Kinetic Energy/Potential Energy/Lagrangian Equation Set,* one obtains the following Lagrangian Equation:

$$L = a^2\Omega^2(m_1 + m_2)sin^2(\Omega t) + 2g[(m_1 + m_2)(a\,cos(\Omega t) + l_1 cos(\phi_1)) + l_2 m_2 cos(\phi_2)]$$
$$+ 2l_2 m_2 \phi'_2[a\Omega\,sin(\phi_2)sin(\Omega t) + l_1 \phi'_1 cos(\phi_1 - \phi_2)] + l_1(m_1 + m_2)\phi'_1(2a\Omega\,sin(\phi_1)sin(\Omega t) + l_1 \phi'_1)$$
$$+ l_2{}^2 m_2(\phi'_2)^2$$

Final Lagrangian Equation

From this *Final Lagrangian Equation*, we can use the known property of the Lagrangian given by:

$$\frac{d}{dt}\left(\frac{\partial L}{\partial \phi_1'}\right) - \frac{\partial L}{\partial \phi_1} = 0$$
$$\frac{d}{dt}\left(\frac{\partial L}{\partial \phi_2'}\right) - \frac{\partial L}{\partial \phi_2} = 0$$

General Equations of Motion

Substituting the *Final Lagrangian Equation* into the given *General Equations of Motion,* we obtain the following 2nd Order ODE equations of motion:

$$(m_1 + m_2)[sin(\phi_1)(a\Omega^2 cos(\Omega t) + g) + l_1 \phi_1''] + l_2 m_2 \phi_2'' cos(\phi_1 - \phi_2) + l_2 m_2(\phi_2')^2 sin(\phi_1 - \phi_2) = 0$$
$$sin(\phi_2)(a\Omega^2 cos(\Omega t) + g) + l_1 \phi_1'' cos(\phi_1 - \phi_2) - l_1(\phi_1')^2 sin(\phi_1 - \phi_2) + l_2 \phi_2'' = 0$$

Final Equations of Motion

After obtaining these *Final Equations of Motion*, we were able to decompose this set of 2nd order ODE equations into 4 simultaneous 1st Order ODE equations, which could then be implemented into the same Python ODE solver used in the Midterm paper. The details of how this was done, and what the final set of ODE equations looked like, is given in the section below.

Modified Python ODE Solver:

Similar to the Midterm Paper, we utilized the RK4 ODE solver. For reference on how this solver was implemented, see the Midterm paper.

The main difference in this Python script was the function being solved for, as the Lagragian that defined the system was much more complex than that of the simple inverted pendulum. In fact, since there were two angles to solve for, there were actually 2 separate 2nd Order ODEs to solve for. Similar to the Midterm paper, we decomposed it such that we essentially were solving for 4 contiguous 1st Order ODEs.

The two equations that we used for such, as highlighted in the previous sections, were as follows:

Define:

$$C = (m_1 + m_2)l_1$$
$$f_1(\phi_1, \phi_2, \phi_2') = (m_1 + m_2)\sin(\phi_1)(a\Omega^2\cos(\Omega t) + g) + l_2 m_2(\phi_2')^2 \sin(\phi_1 - \phi_2)$$
$$g_1(\phi_1, \phi_2) = l_2 m_2\cos(\phi_1 - \phi_2)$$
$$f_2(\phi_1, \phi_2, \phi_1') = a\Omega^2\cos(\Omega t)\sin(\phi_2) + g\sin(\phi_2) - l_1(\phi_1')^2\sin(\phi_1 - \phi_2)$$
$$g_2(\phi_1, \phi_2) = l_1\cos(\phi_1 - \phi_2)$$

Equations Set A

Using Equation Set A:

$$\phi_1'' = \frac{\frac{1}{Cl_2}f_2(\phi_1,\phi_2,\phi_1')g_1(\phi_1,\phi_2) - \frac{1}{C}f_1(\phi_1,\phi_2,\phi_2')}{1 - \frac{1}{Cl_2}g_1(\phi_1,\phi_2)g_2(\phi_1,\phi_2)}$$

$$\phi_2'' = \frac{\frac{1}{Cl_2}f_1(\phi_1,\phi_2,\phi_2')g_2(\phi_1,\phi_2) - \frac{1}{l_2}f_2(\phi_1,\phi_2,\phi_1')}{1 - \frac{1}{Cl_2}g_1(\phi_1,\phi_2)g_2(\phi_1,\phi_2)}$$

Equations of Motion for ϕ_1 and ϕ_2

The set of First Order ODE systems that corresponds to these 2nd Order ODEs was:

$$u = \phi_1$$
$$v = u' = \phi_1'$$
$$p = \phi_2$$
$$q = p' = \phi_2'$$

Equations Set B

$$u' = \phi_1' = v$$
$$v' = \phi_1'' = \frac{\frac{1}{Cl_2}f_2(\phi_1,\phi_2,\phi_1')g_1(\phi_1,\phi_2) - \frac{1}{C}f_1(\phi_1,\phi_2,\phi_2')}{1 - \frac{1}{Cl_2}g_1(\phi_1,\phi_2)g_2(\phi_1,\phi_2)}$$
$$p' = \phi_2' = q$$

$$q = \phi_2'' = \frac{\frac{1}{Cl_2}f_1(\phi_1,\phi_2,\phi_2')g_2(\phi_1,\phi_2) - \frac{1}{l_2}f_2(\phi_1,\phi_2,\phi_1')}{1-\frac{1}{Cl_2}g_1(\phi_1,\phi_2)g_2(\phi_1,\phi_2)}$$

First Order ODE Equation Set

Similarly to the Midterm paper, there were a number of initial parameters that were defined earlier in the code. Of course, however, there are now two masses and two arm lengths defined within the system:

This code then gave us ϕ_1 vs. t, ϕ_1' vs. t, ϕ_2 vs. t, ϕ_2' vs. t plots. A set of these plots for the initial conditions of $\phi_1 = 0.5$ radians and $\phi_2 = 0.5$ radians is shown in Figures 2 through 6:

Figure 3. ϕ_1 *vs t*

Figure 4. ϕ_1' *vs t*

Figure 5. ϕ_2 *vs t*
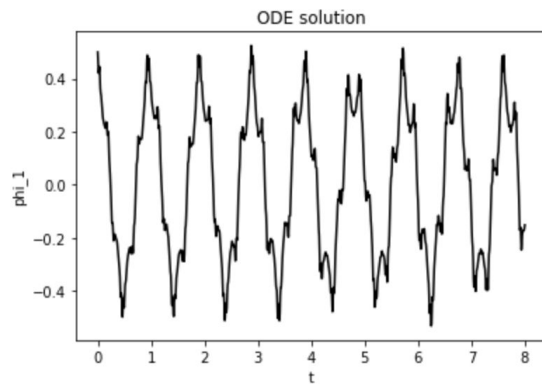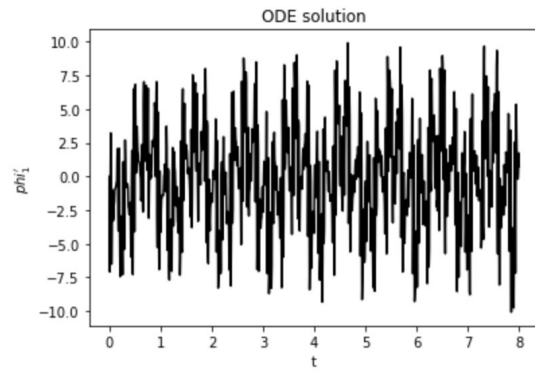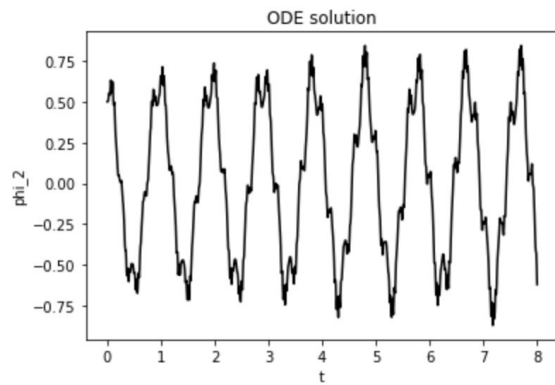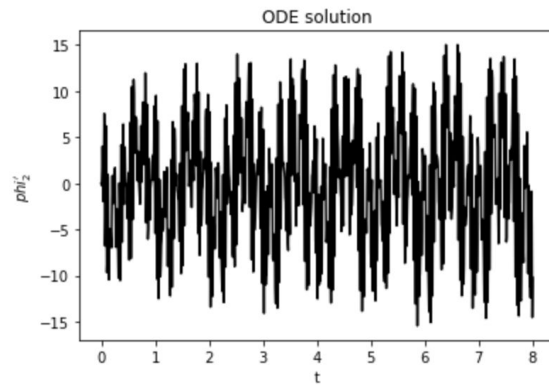
Figure 6. ϕ_2' *vs t*

However, these were extremely hard to interpret on their own, and it was clear we would need an additional resource to help us visualize what these plots were telling us. For this, we used a modified Double Pendulum simulator, as described in the section below.

Pendulum Motion Simulator:

As mentioned previously, the various plots that we obtained for the different angles of the arms did not provide an adequate visual demonstration of the system. Therefore, we decided to spend some time working with another open source Python script that could model this DIP motion.

We obtained the initial Python script from a website that provided the resources to model a standard Double Pendulum (insert reference footnote here). This initial script was very convenient to have, as it already gave us the tools to observe the animation of the system.

We then only needed to modify the equations of motion set in the derivative function to match the DIP system's equations of motion, and then additionally modify the x and y coordinate equations to include the oscillation of the base. The program then would use the RK4 ODE solver on the system, generate a large set of images representing the DIP system at that time step, and save these all to a single directory. Then an additional Python built-in function was used to compile these images into a single GIF file that described how the pendulum was moving in a small video segment.

To demonstrate this to some extent, we added a Cartesian plot of the ends of each of the arms. In the plot below, the black lines at the bottom represent the position of the end of the first arm, and the red dots represent the position of the end of the second arm in the system.
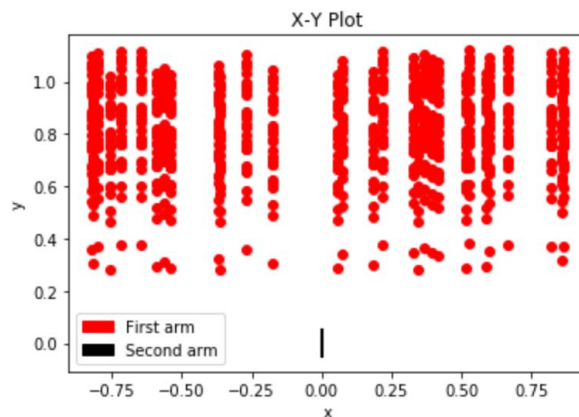
Figure 7. Cartesian plot of two ends of arms

When observing the corresponding GIF file produced by the simulator, this plot tends to make sense. This is because the plot above corresponds to the first couple of seconds of this system, and when observing the GIF simulation they correspond to the initial trajectory quite well. The initial movements of the pendulum system are very short and small at the end of the first arm, which oscillates about the upward vertical stable point slowly, while the end of the secondary arm oscillates much more rapidly over a much larger X and Y range. While not all of these details are ingrained in the plot above, one can better understand the overall movements of the pendulum much more so than with the ϕ_1 vs. t and ϕ_2 vs. t plots shown from Figures 3 through 6.

Verification of Simulator:

One important point to verify in this entire process was the validity of the plots and of the simulation results being obtained from these Python scripts. Because we did not have our own DIP system at our disposal, due to the pandemic, we did not have a physical system that could verify the results we were obtaining from these programs. Therefore, we needed another method of ensuring (to the best of our abilities) that the results seen were consistent with what we would expect.

The question was how we would go about doing this without any physical system at our disposal. We decided to analyze the system with a much larger l_1 and m_1 values as compared to the l_2 and m_2 values. This is because such a system would tend to behave similar to the single inverted pendulum, a system we had studied extensively for our previous research paper. Additionally, while we also did not have a physical inverted pendulum system for the previous research paper, we had several articles that detailed the analysis of an inverted pendulum system, and they had identical equations of motion associated with their systems. Therefore, since we were quite certain our initial Inverted Pendulum plots were accurate, we could compare the DIP plots with the conditions as described above with those of the Inverted Pendulum with the same parameters.

The plots in Figures 8 through 10 came from the original, single inverted pendulum system with an initial condition of $\theta = 1$ radians:

Figure 8. θ vs t
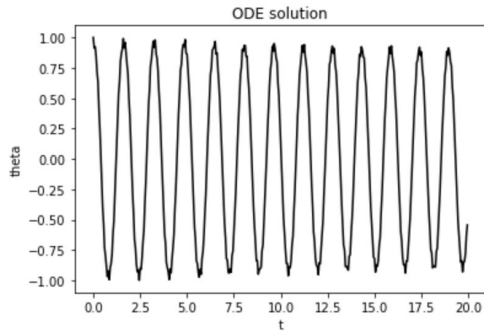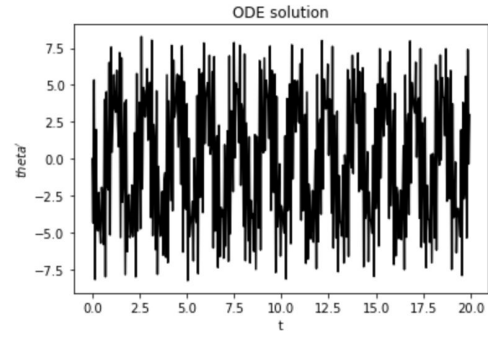
Figure 9. θ′ vs t
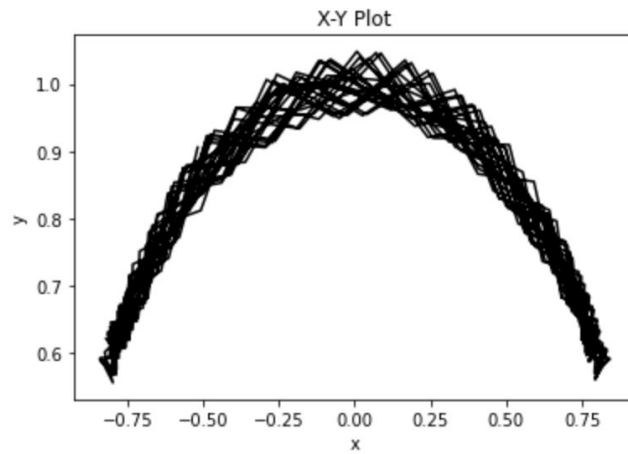
Figure 10. Cartesian plot of arm movement

Then, the DIP system was set with the following parameters to mirror this single inverted pendulum system:

$$m_1 = 1\,g$$
$$m_2 = 0.1\,g$$
$$l_1 = 1\,m$$
$$l_2 = 0.1\,m$$
$$a = 0.05\,m$$
$$\Omega = 180\,Hz$$
$$g = 9.1\,\frac{m}{s^2}$$

DIP parameters to mirror single Inverted Pendulum

Then when running the ODE solver made for the DIP system, the ϕ_1 vs. t, ϕ_1' vs. t, ϕ_2 vs. t, ϕ_2' vs. t plots are shown in Figures 11 through 14:
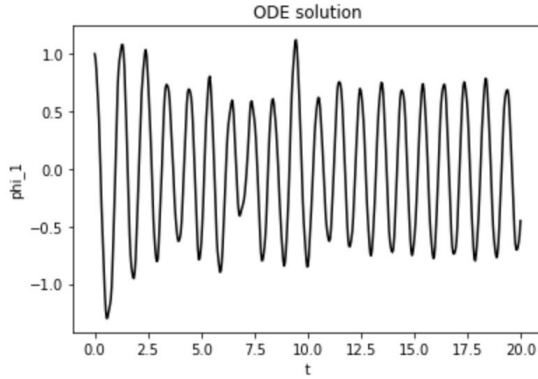
Figure 11. ϕ_1 vs t
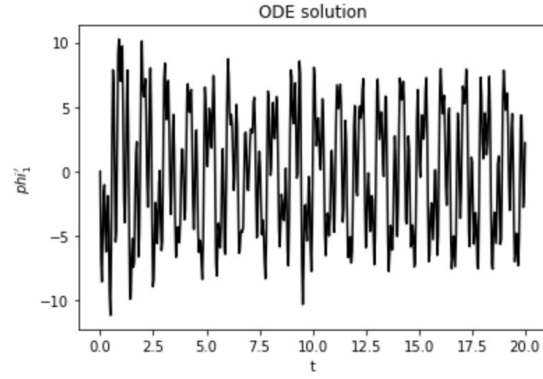
Figure 12. ϕ_1' vs t
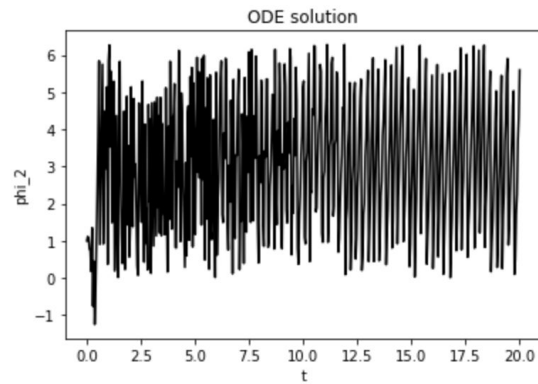
Figure 13. ϕ_2 vs t
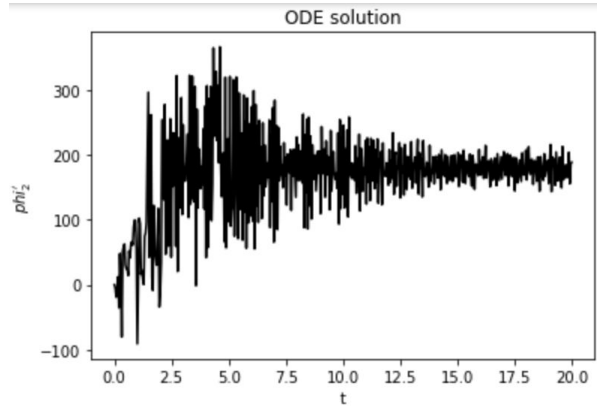
Figure 14. ϕ_2' vs t

As seen in the Figure 9 and Figure 10 plots, the ϕ_1 vs. t and the ϕ_1' vs. t mirror the single inverted pendulum quite closely. There are slight discrepancies in the two sets of plots, and this makes some sense, as the secondary pendulum arm will tend to have some effect on the movement of the first arm, no matter how small the arm is and how light the mass is.

The plots in Figure 11 and Figure 12 showing the ϕ_2 vs. t and ϕ_2' vs. t show how rapidly the second arm oscillates around the first, but was not of much importance in this section of the analysis.

Finally, the Cartesian plot was created for this system, to better understand if indeed the DIP system constructed roughly matched that of the single Inverted Pendulum system. As seen

in Figure 15, the movement of the first arm (shown in red) was roughly consistent with what was predicted by the single Inverted pendulum:
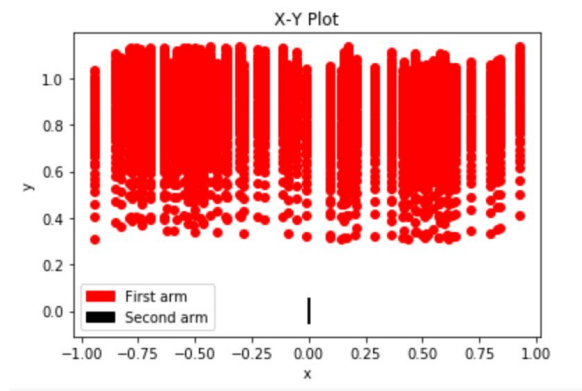
Figure 15. Cartesian plot of arm movement for DIP

Analysis of Stability of DIP:

To analyze the stability of the double pendulum we first want to look at what happens when we start the pendulum at different locations and observe how it moves under these conditions and if points of stable equilibrium become evident. For this we will first use our normal system setup, $m_1 = m_2 = 1\ gram$, $l_1 = l_2 = 1m$, amplitude of base (a) = .08 m, frequency of base = 190Hz and observed over an 8 second interval. For this first graph we used initial conditions of $\phi_1 = 0\ radians$ and $\phi_2 = 0\ radians$ which is a stable equilibrium point both for the inverted pendulum and a regular pendulum.
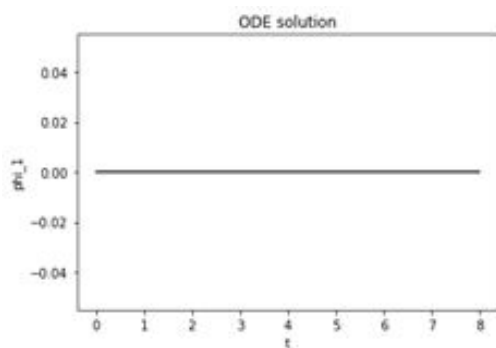
Figure 16. ϕ_1 vs t
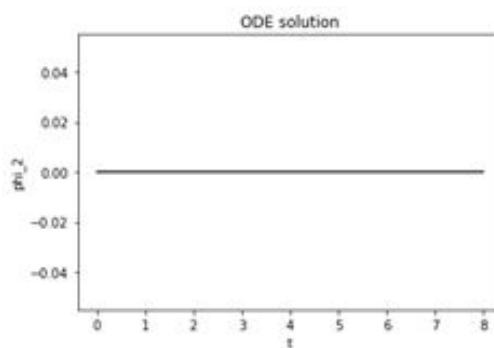
Figure 17. ϕ_2 vs t
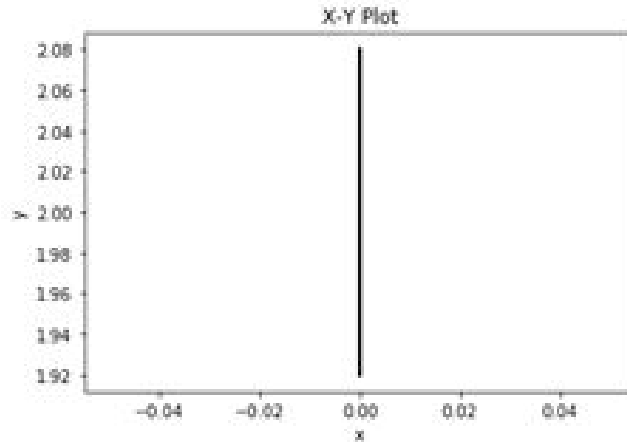
Figure 18. X/Y Plot

From these three graphs we see that when both pendulums start in the downward equilibrium point the system remains stable and neither of the pendulums move from this position. This, while trivial, reveals that the solver does work for the trivial situation of both in this position.

The next test case is when they are both vertical (a stable equilibrium point for the single inverted pendulum):
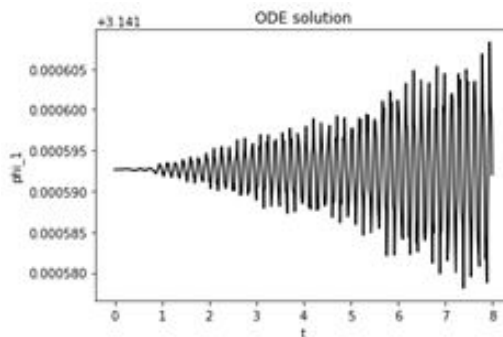
Figure 19. ϕ_1 *vs t*
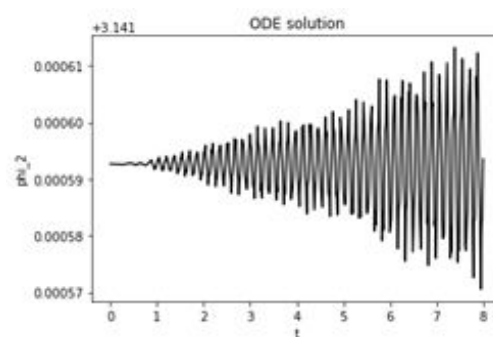
Figure 20. ϕ_2 *vs t*
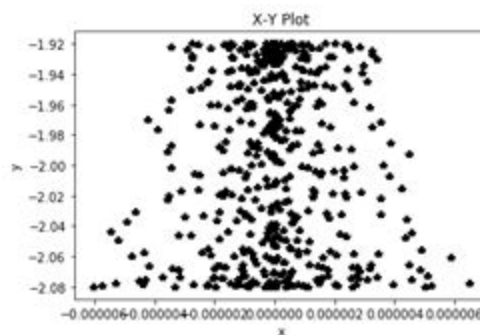
Figure 21. X/Y Plot

From these three figures above we observe that when both arms start in the vertical position that they both stay relatively upright, however they oscillate about the vertical with increasing amplitude. This is most likely a result of the momentum from each previous swing to the side being conserved and the energy transferring from the bottom to the top. However, this point still remains a stable equilibrium point as the amplitude of the oscillations is quite small and would take time to fully deteriorate.

Next we want to look at a situation where the bottom pendulum is at a stable equilibrium point and the second arm is not. For this we have arm one start at the vertical down and the second arm is positioned at the right horizontal (an unstable equilibrium point for normal inverted pendulum):
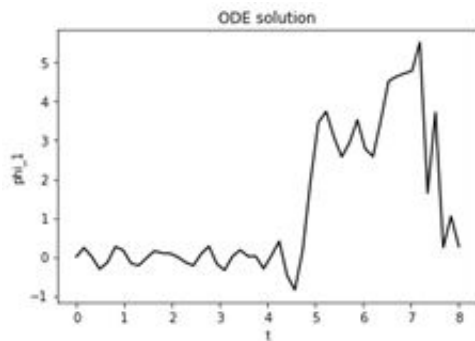
Figure 22. ϕ_1 vs t
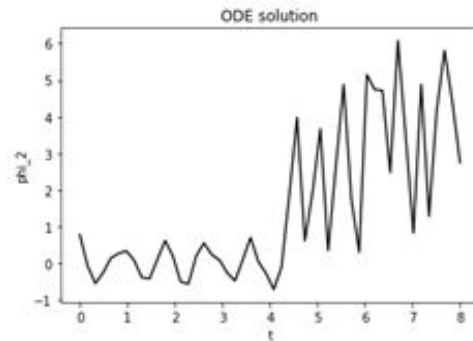
Figure 23. ϕ_2 vs t
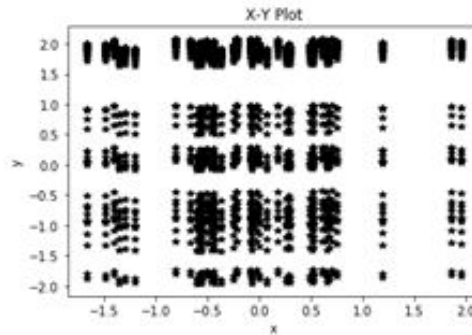
Figure 24. X/Y Plot

From these three graphs we observe that there exists some equilibrium for the first arm about the bottom at the start, and then momentary equilibrium at the top position before falling out of equilibrium state. For the second arm we see it also oscillate about the bottom point but then begins to continue to increase in angle during oscillation amplitude over time.

Next we look at when both start at an unstable equilibrium point (horizontally right):
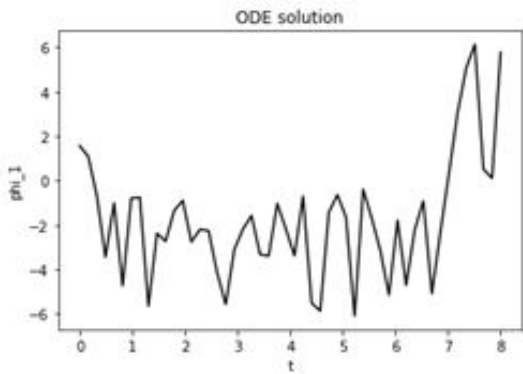
Figure 25. ϕ_1 *vs t*
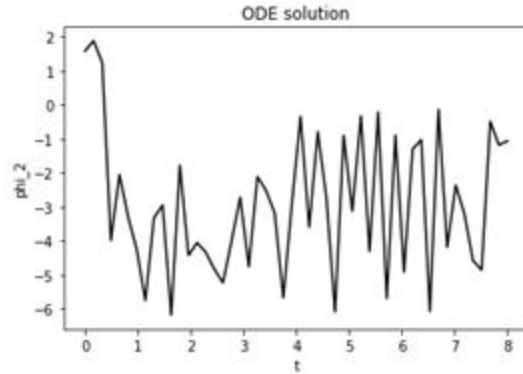
Figure 26. ϕ_2 *vs t*
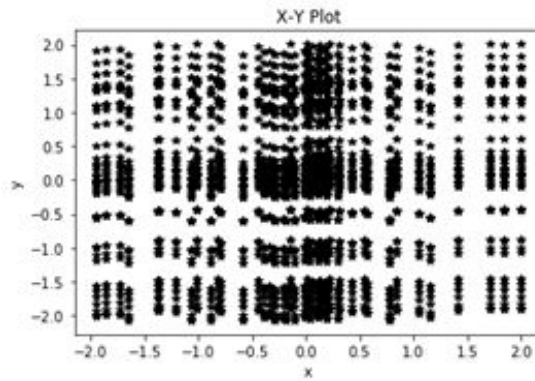
Figure 27. X/Y Plot

In these three graphs we see much more chaotic motion and observe that they do not gravitate towards any particular equilibrium point except the first arm tends to oscillate about the vertical position while the second arm seems to move much more chaotically.

Finally we wanted to look at what happens when you put the first at a non equilibrium point and the other anywhere. For this we start with arm one at 3pi/4 and the second arm at pi/2 (horizontal right):
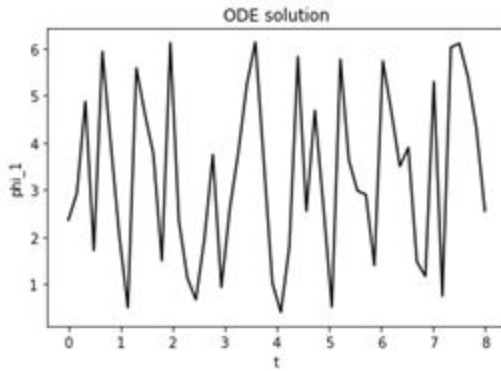
Figure 28. ϕ_1 vs t
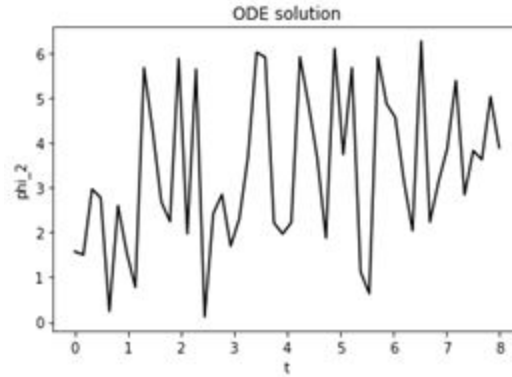
Figure 29. ϕ_2 vs t
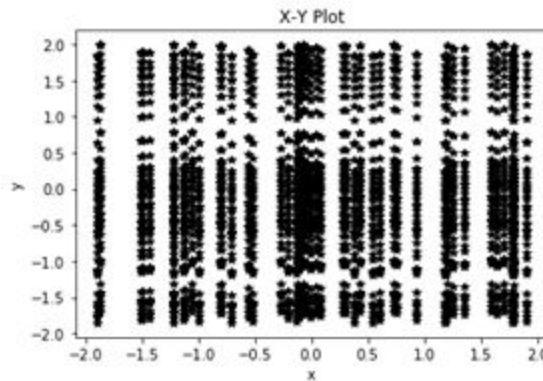
Figure 30. X/Y Plot

From these graphs we found that they move extremely chaotically and do not tend towards either equilibrium points, which we would expect because this was the observed case in the single inverted pendulum. The initial conditions for each of these tests were starting the first arm at the down vertical position and the second is at unstable equilibrium at the horizontal right position.

Now we want to look at the stability of the system, and to do this we wanted to look at various combinations of arm lengths and point mass values and analyze both graphically and through simulation the effect on the system. To start we will have initial conditions such that; the length of the first and second rod is equal to 1 meter, the mass on both is 1 gram, the amplitude of the vibrating base is .08 meters, and the frequency is 190 Hz. From here we will try some combinations of lengths of l1 and l2, starting with 2:1, then 10:1, then 100: 1 followed by the inverse of these; 1:2, then 1:10, then 1:100.

First we want to show the base system when the lengths are equal at 1 meter:
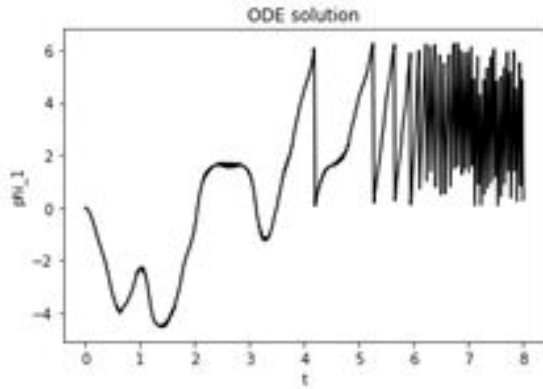
Figure 31. ϕ_1 *vs t*
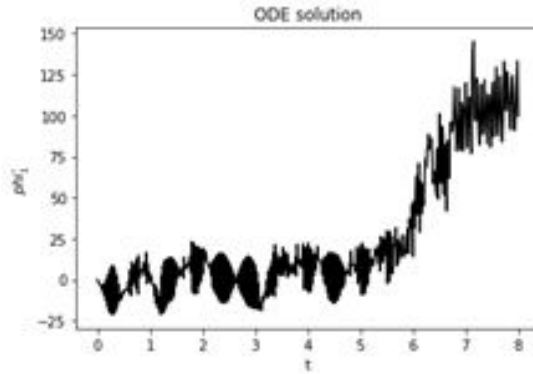
Figure 32. ϕ_1' *vs t*
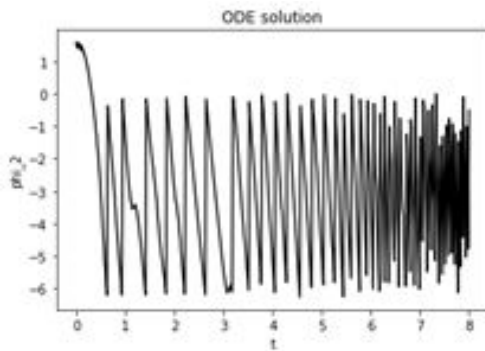
Figure 33. ϕ_2 *vs t*
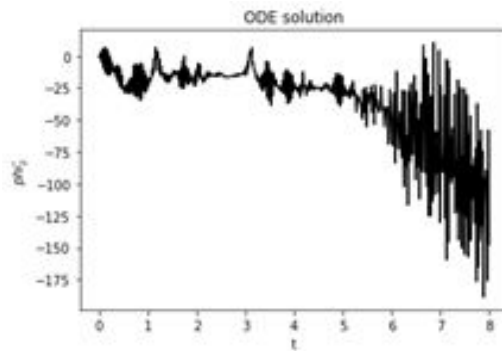
Figure 34. ϕ_2' *vs t*
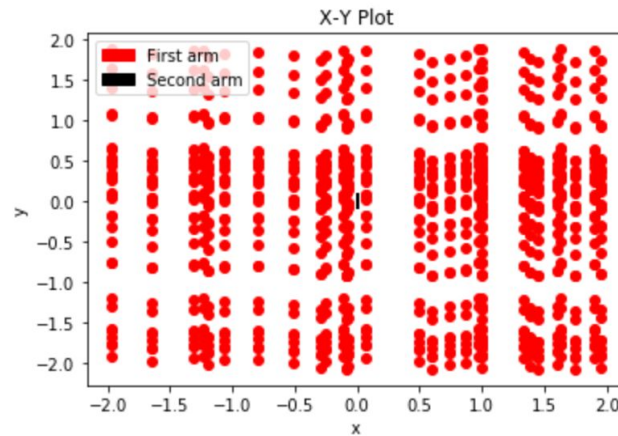
Figure 35. X/Y Plot

Looking at Figures 16 through 19, we are able to piece together a picture of what is actually going on in this combination of arm lengths. We see that there is a somewhat chaotic motion to the first angle for the first few seconds, but then its motion becomes much more sinusoidal. The second angle ϕ_2 starts off relatively oscillatory with various striations from sinusoidal. Based on the graphs we see that ϕ_2 oscillates about the angle -3 radians (

approximately π radians) while ϕ_1 oscillates about π radians as well once it appears to reach equilibrium motion. This would mean that both oscillate about the vertical down position, the natural resting point of a plain pendulum.

Now to look at a ratio of L1:L2 of 2:1
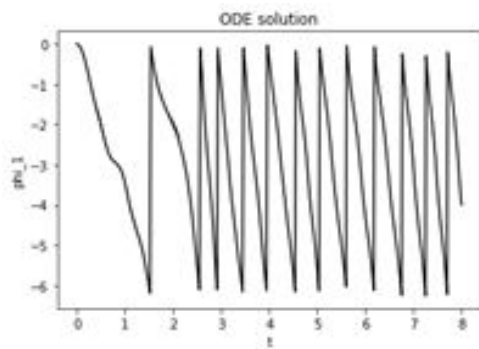
Figure 36. ϕ_1 *vs t*
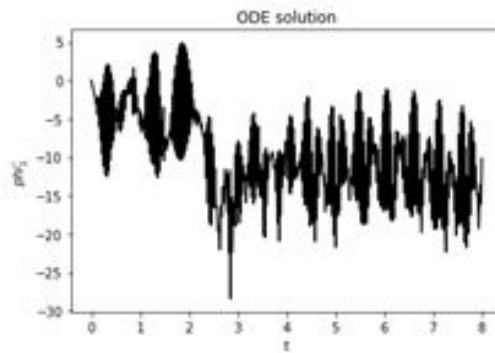
Figure 37. ϕ_1' *vs t*
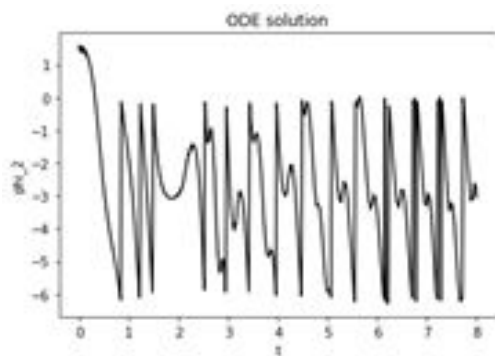
Figure 38. ϕ_2 *vs t*
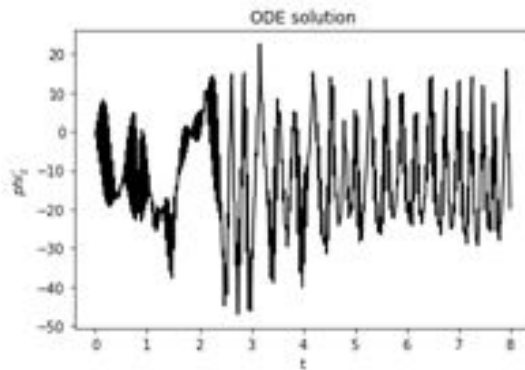
Figure 39. ϕ_2' *vs t*
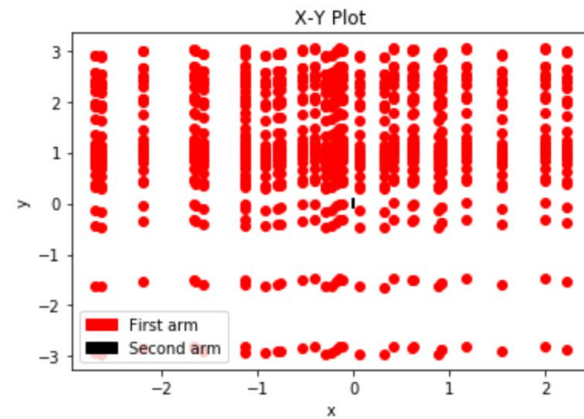
Figure 40. X/Y Plot

In Figures 21 through 24, we observe that by doubling the length of arm 1 we drastically change the system's response and see that ϕ_1 has a much more oscillatory pattern but with more sharp movements. ϕ_2 still oscillates around π but does so more chaotically.

Next we observe the 10:1 ratio
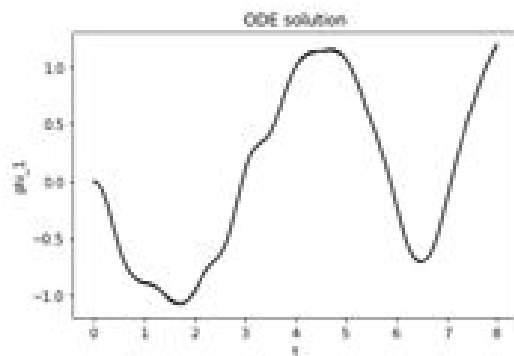
Figure 41. ϕ_1 vs t
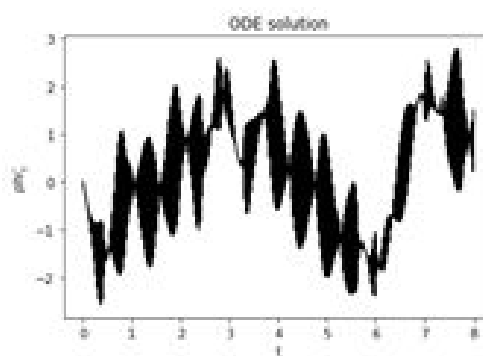
Figure 42. ϕ_1' vs t
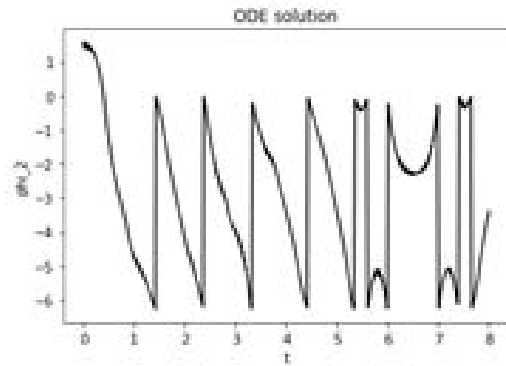
Figure 43. ϕ_2 vs t
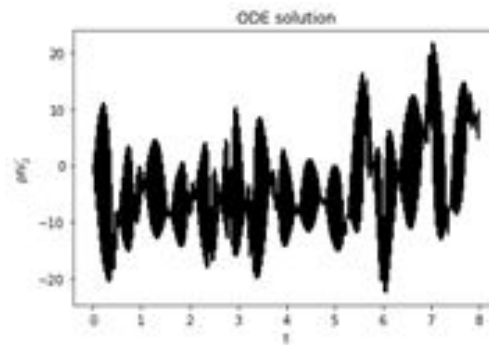
Figure 44. ϕ_2' vs t
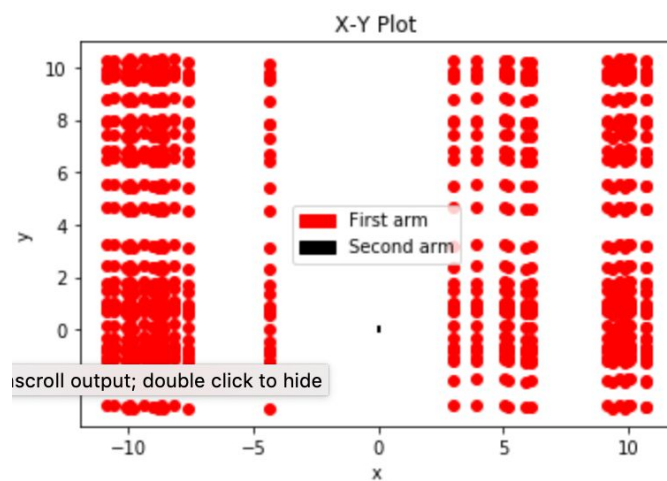
Figure 45. X/Y Plot

Looking at the 10:1 ratio we see that the first arm becomes more difficult to rotate and so we see less change for ϕ_1. However for this graph the ϕ_1' vs ϕ_1 gives us something that we have sort of seen before:
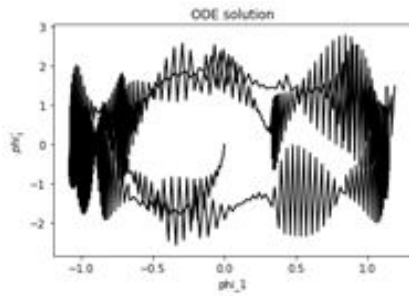
Here in Figure 46 we see a graph that resembles the graph of the single inverted pendulum, and when run under simulation we see that it begins performing closer to the single pendulum, meaning it has points of stability at the top and bottom positions. This time however the addition of the second arm allows the pendulum to gain more angular momentum and thus spin faster each time.

Figure 46. ϕ_1 *vs* ϕ_1'

When we increased the ratio even more to 100:1 we found an odd result where the pendulum starts by rocking slightly and then travelling around in a full circle continuously. The graphs looked like this:
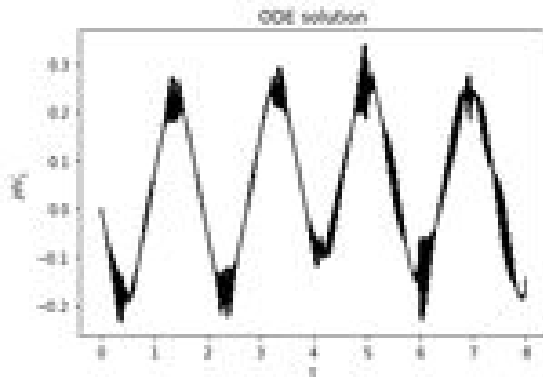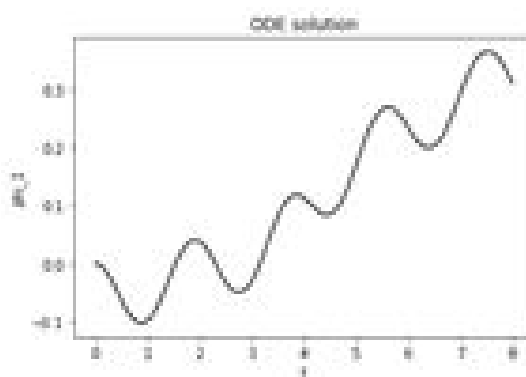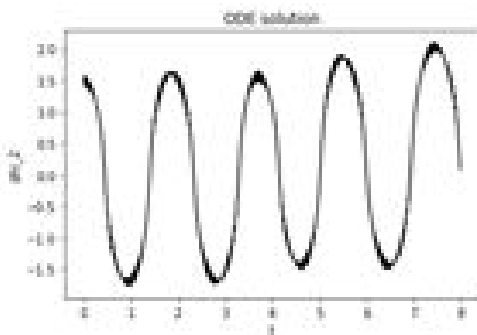

Figure 47. ϕ_1 *vs t*

Figure 48. ϕ_1' *vs t*
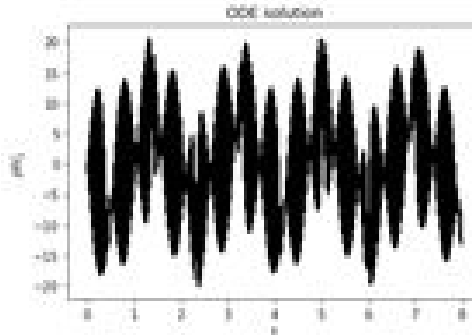

Figure 49. ϕ_2 *vs t*
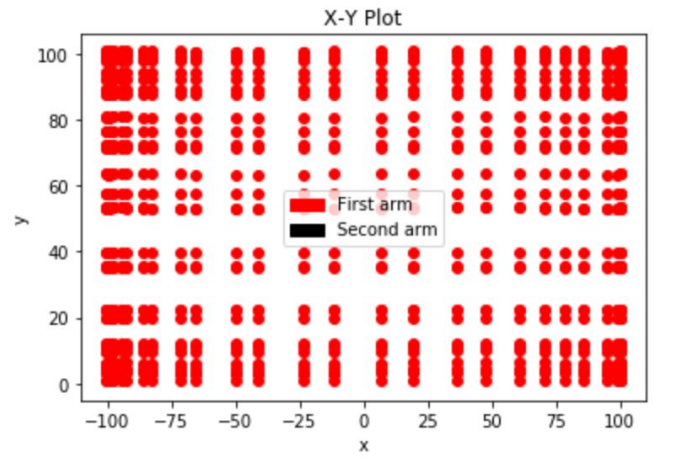

Figure 50. ϕ_2' *vs t*

Figure 51. X/Y Plot

It was interesting to see that for both angles the curves were quite smooth, and that when run under simulation the system as a whole seemed relatively stable.

Next we wanted to see if the order of the arms lengths made a difference so we repeated these tests but with L2 being increased instead of L2.
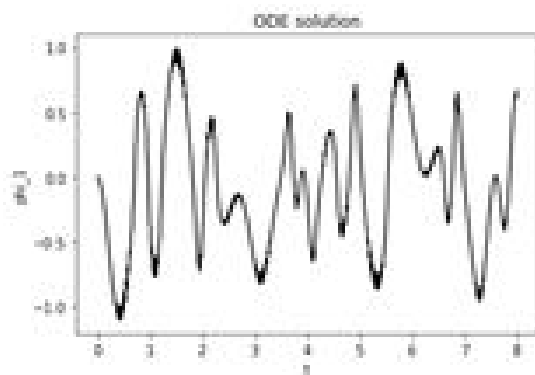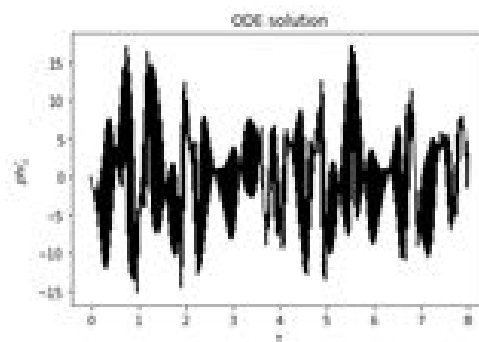
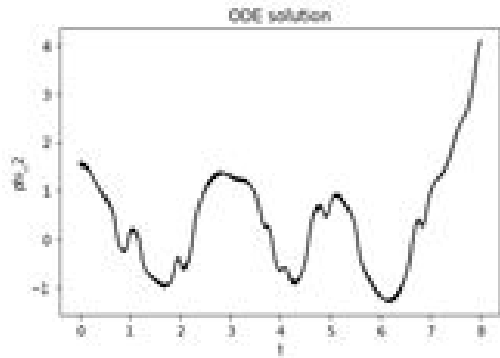For L2 = 2, we get:

Figure 52. ϕ_1 *vs t*

Figure 53. ϕ_1' *vs t*
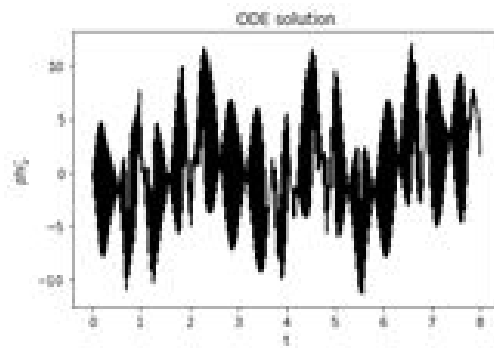
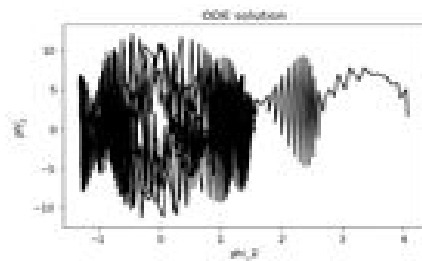Figure 54. ϕ_2 vs t

Figure 55. ϕ_2' vs t

Figure 56. ϕ_1 vs ϕ_1'

What is interesting about this case is that it appears to have more stability than when the L1 was 2 instead. However the motion of the arms was more chaotic but there seemed to still exist equilibria.
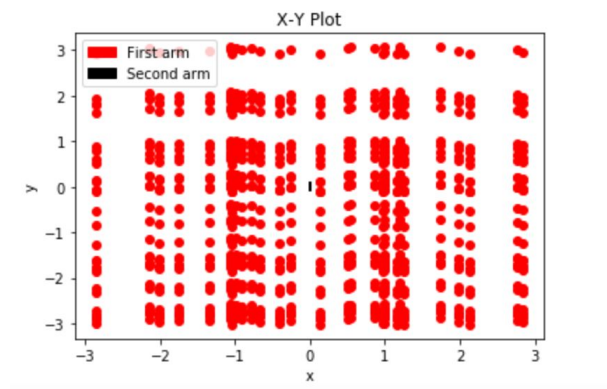

Figure 57. X/Y Plot
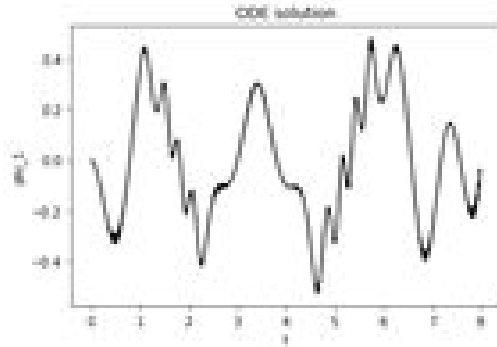
Now we will look at when L2 = 10:

Figure 58. ϕ_1 vs t

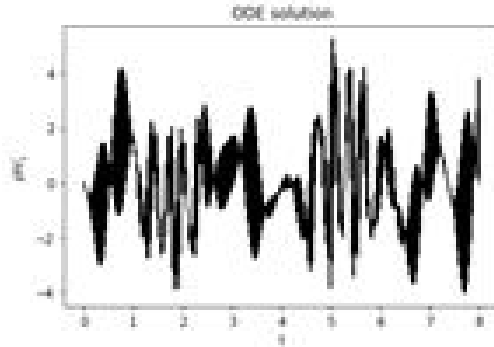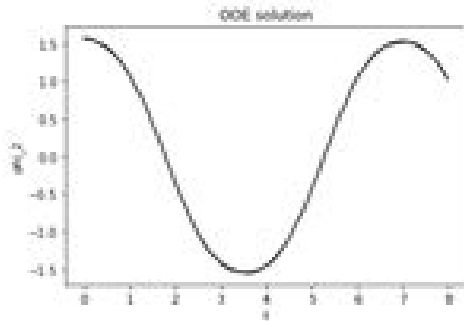Figure 59. ϕ_1' vs t

Figure 60. ϕ_2 vs t
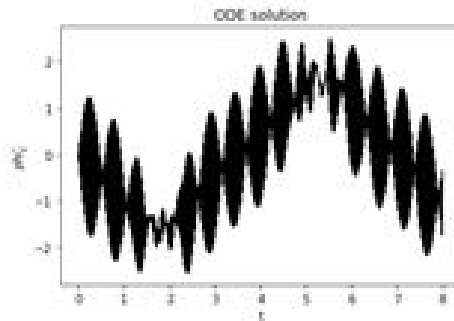
Figure 61. ϕ_2' vs t

In this situation we see an interesting result in the motion of ϕ_2 as it is a smooth sinusoidal curve and ϕ'_2 is also sinusoidal which is interesting in that we can see that some equilibrium points start to develop. This is also more evident in the ϕ_2' vs ϕ_2 graph:

Figure 62. ϕ'_2 vs ϕ_2

Figure 63. X/Y Plot

From these two graphs we see that there is a much nicer equilibrium for the second arm that tends to oscillate about 0 radians.

Finally we have the graphs of the 1:100 ratio:

Figure 64. ϕ_1 vs t

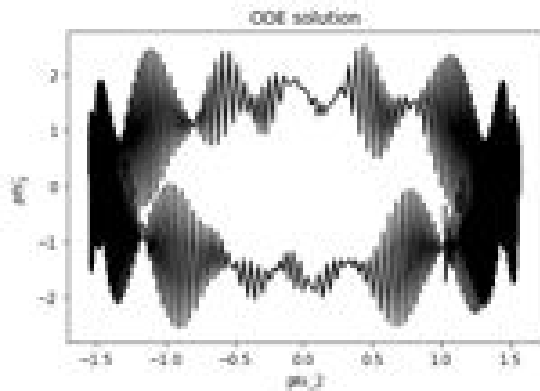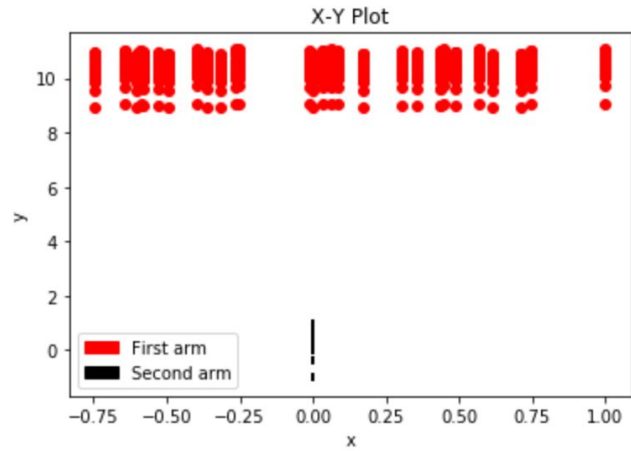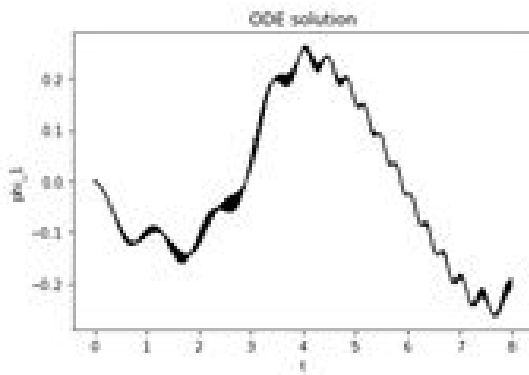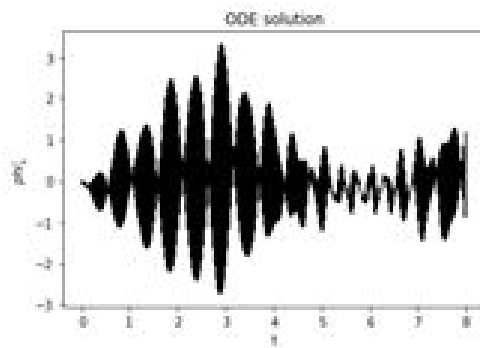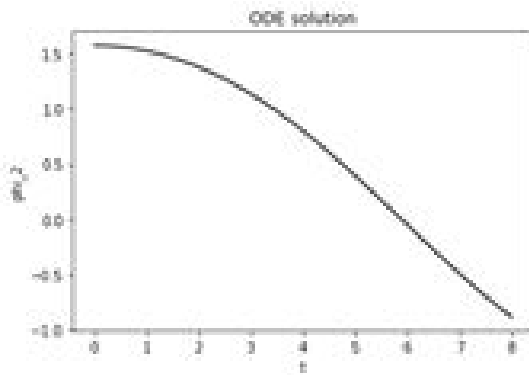Figure 65. ϕ_1' vs t
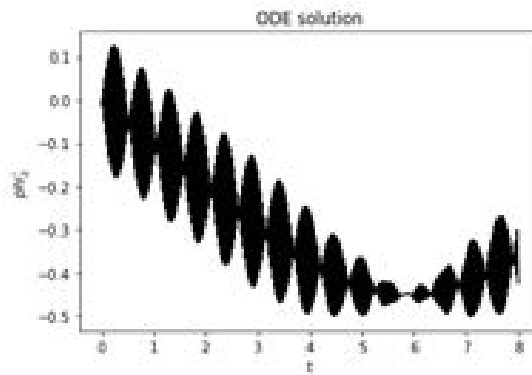

Figure 66. ϕ_2 vs t
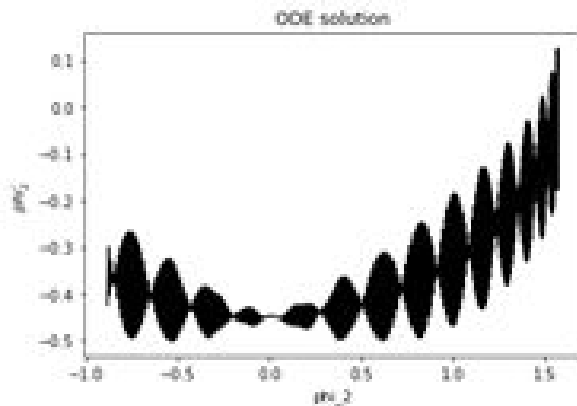

Figure 67. ϕ_2' vs t

Figure 68. ϕ_1 *vs* ϕ_1'

     From the graphs above we see that there was an odd motion from the second arm as it did not complete one full period of oscillation as the others before had done. This was a result of the arm being significantly longer than the amplitude of oscillation of the base. When I tested it with a higher amplitude I found that it acted much more similarly to the 1:10 ratio and approached the motion of the single inverted pendulum.

Conclusion:

     Our primary goal for modeling the DIP system was to attempt to derive a process for finding the stable points of the system. Unfortunately, with the limited time and multiple obstacles that our team faced, we were unable to accurately obtain a process for finding stable points of the system.

     We did, however, achieve some of what we were hoping to finish. We were able to derive the Lagrangian equation and Equations of Motion that defined the DIP system we analyze, which was different from any of the other DIP systems we found in research papers. This was because the majority of the other DIP systems explored in research papers analyzed the Double Pendulum arm system on a base that was moving in the X direction, not oscillating in the Y direction.

     We were also able, to some degree, verify that the equations we obtained were accurate. This was because we were able to construct a system that would theoretically behave very similarly to a Single Inverted Pendulum, of which we had studied thoroughly in the Midterm paper. We also had several papers that arrived at the same Lagrangian equation for the Single Inverted Pendulum that we had, so we were fairly certain that our Python simulator was accurate

for this system. When we performed this analysis on the ϕ plots of the DIP system, we observed that the ϕ_1 *vs t* plots were essentially identical, giving us a reason to believe our DIP simulator, which utilized the Lagragian equations we derived, were indeed accurate.

Our analysis of the DIP system with various different lengths of the two arms gave us some idea of how this parameter affected the movements of the overall system. We hoped that this analysis could display how these plots changed with different system parameters, and then apply these findings to a generalized system. We found that by changing initial conditions of the system while keeping the base parameters intact that the double inverted pendulum tended to act similarly to the single inverted pendulum in some interesting ways. For one, the first arm usually tended to act the most like the single pendulum and would tend towards certain points of stability, and thus the second arm was dependent on the first arm approaching equilibrium. When the first tended towards the unstable equilibrium, the motion of the whole system became quite chaotic.

After this we looked at the pendulum with changing the starting parameters, specifically length of the arms. We found that as one arm became significantly longer than the other, the system tended to act more like the single inverted pendulum. We also found that the order for this operation did matter, as the same ratio but different orders often yielded different results. This is most likely due to how the second arm's motion is dependent on the first more than the first is dependent on the second.

This provides a clear path for potential future work. If we thoroughly analyze the various stability points of different systems, we would have the ability to apply a rough estimation theory to the system, as many of the other research papers were able to do. This would provide an estimation theory that could be applied to systems that oscillate in the vertical direction rather than traverse in the horizontal direction. These estimation theories could then be used for more advanced systems with more complex Equations of Motion that are primarily affected by oscillations in the vertical direction.

Another analysis that we looked at but did not include was looking at the effect of changing the masses of the pendulums in different ratios and orders. A brief analysis for this found that with greater ratios of weights the system would act quite strange, the most notable being that it would often "snap" one of the arms a particular direction and have a very high angular frequency and angular acceleration. This is to be expected as this would be modelling a basic "whip" type motion, meaning when the first mass was much greater its momentum is quite great resulting in the whipping of the second mass to conserve momentum.

Further in the future we would want to look at all these changes (length and mass) as well as frequency and amplitude of the base and look at various initial conditions to see if the stability of the system changes.

References:

1. B. Xu, Y. Lyu, S. Gadsden, "Estimation and Control of a Double-Inverted Pendulum", CSME International Congress, 1-6 (2018)

2. K. Srikanth, G. Kumar, "Stabilization at Upright Equilibrium Position of a Double Inverted Pendulum with Unconstrained BAT optimization", International Journal on Computational Science and Applications, 1-15 (2015)

3. Q. Li, W. Tao, C. Zhang, "Stabilization Control of Double Inverted Pendulum System", IEEE, 1-8 (2008)

4. H. Niemann, J. Poulsen, "Design and Analysis for Controllers for a Double Inverted Pendulum", ISA Transactions, 145-163 (2005)

5. Christian, "The Double Pendulum", https://scipython.com/blog/the-double-pendulum/, (2017)